

Large-scale friction and wear tests on a hybrid UHMWPE-pad/primer coating combination used as bearing element in an extremely high-loaded ball-joint

P. Samyn^{a,*}, L. Van Schepdael^b, J.S. Leendertz^c, A. Gerber^d,
W. Van Paepegem^a, P. De Baets^a, J. Degrieck^a

^aDepartment Mechanical Construction and Production, Laboratory Soete, Ghent University, St Pietersnieuwstraat 41, B-9000 Gent, Belgium

^bSOLICO B.V., Solutions in Composites, Everdenberg 97, NL-4902 TT Oosterhout, The Netherlands

^cMinistry of Transport, Public Works and Water Management, Directorate-General, Herman Gorterhove 4, NL-2700 AB Zoetermeer, The Netherlands

^dUniversity of Stuttgart, Staatliche Materialprüfungsanstalt, G-70550 Stuttgart (Vaihingen), Germany

Available online 10 August 2005

Abstract

The surfaces of a heavily loaded ball-joint were initially covered with a sliding spray and suffer wear. A solution is found by incorporating UHMWPE pads (Ultra high molecular weight polyethylene) with a carbon fibre/epoxy reinforced ring as sliding material into the chairs of the structure, while the steel ball-side is covered with a Zn-phosphate primer coating, protecting against corrosion. The local static and dynamic behaviour of the hybrid UHMWPE pads in contact with steel or Zn-coated counterfaces has been large-scale tested on loading capacity, low friction and wear resistance. For protection of the sliding counterface against wear, a polymer lip covering the carbon ring has been experimentally designed to flow over the carbon ring under high contact pressures, assuming the retained polymer disc under hydrostatic conditions. As such, the soft coating resists extremely high contact pressures (150 MPa) with good adhesion to the steel ball. However the application method should be carefully selected, sprayed coatings are the most favourable for low initial static friction. Calculated bulk and flash temperatures revealed that the UHMWPE melting temperature is not exceeded, although softening of the coating under high contact pressures may be favourable for a 'self-repairing' ability. Pre-sliding creep and intermediate wear paths as manifesting in the ball-joint were simulated, indicating that the maximum design coefficient of friction is not exceeded. Test results are compared to FEM-calculations to verify the practical applicability of the modified sliding system.

© 2005 Elsevier Ltd. All rights reserved.

Keywords: Large-scale testing; Hybrid UHMWPE pad; Soft coating; Tribology

1. Introduction

Protecting the lands below sea level from being flooded by water requires the construction of dikes and surge barriers. A flexible protection is needed near harbours, providing access to container ships without any height restriction. One solution is found in the construction of a movable retaining wall, consisting of two floating hemispherical gates which can be swung from the banks into the river and sunk on the river bed, as e.g. in the Nieuwe Waterweg near Rotterdam. The retaining walls consist of orthotropic plate structures

and are connected to pivots by means of two triangular space trusses made of tubular sections. The rotation and closure of the wall in case of a storm implies horizontal and vertical movements, guaranteed by a pivot or ball-joint with a diameter of 10 m and a weight of 680 tons in the abutments of the structure. The convex and concave ball-joint surfaces were originally (1991) covered with one 10 µm thick layer that is a mixture of MoS₂ and PTFE resin, in order to obtain low friction. For running-in purposes an additional layer of PTFE-spray has been applied to overcome static friction. After several sliding steps the coating was however removed from the contact zone and severe wear marks as cold welding spots were observed due to adhesive steel/steel contact. The modified design finished in 2004 (Fig. 1) contains a primer coating on the convex steel ball surfaces protecting against corrosion and 468 polymer discs or 'pads' incorporated in holes machined into the concave surfaces. The pads have

* Corresponding author. Tel.: +32 9264 3308; fax: +32 9264 3295.

E-mail address: pieter.samyn@ugent.be (P. Samyn).

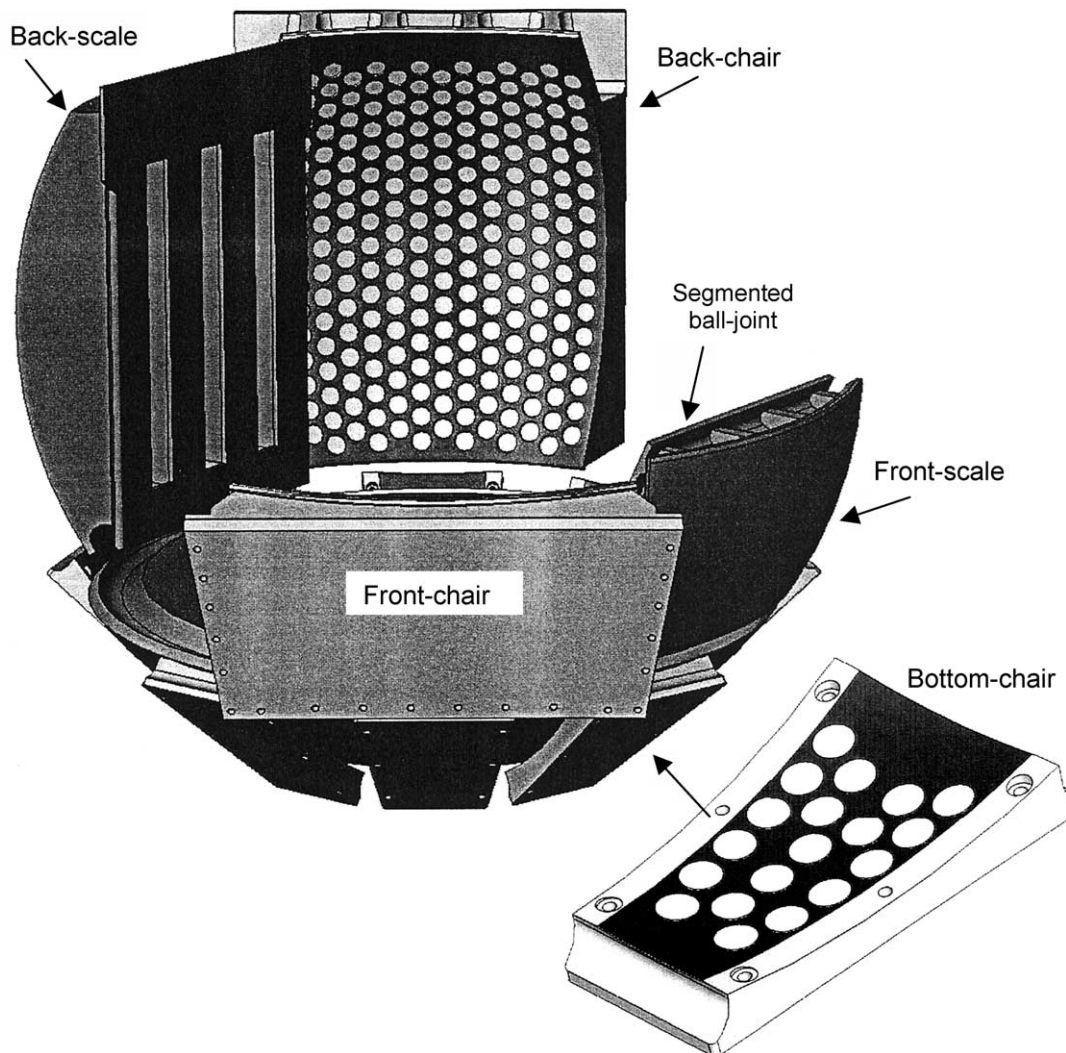


Fig. 1. Modified ball-joint with machined holes ($\text{\O} 250 \text{ mm} \times 32 \text{ mm}$) on the back, front and bottom chairs for incorporation of polymer discs.

a nominal diameter of 249 mm and a thickness of 40 mm, positioned into holes of 250 mm diameter and 32 mm depth. As such, the pads have a free surface of 8 mm above the steel surface and the difference in curvature radii of concave and convex surface is reduced from 20 to 10 mm. Those modifications were analysed in combination with the elasticity, compressibility and thickness of the pads, as they determine the stiffness of the interface.

1.1. Functionality of the ball joint

The shape of the faceted ball-joint is achieved by a rectangular kernel on which two convex cast steel elements are bolted, respectively, the back and front scales, in contact with fixed front and back chairs. The bottom of the kernel contains a bearing element with the shape of a convex ring that rests into eight concave bottom scales fixed to a foundation. During a closure operation as defined in Ref. [1]

the bottom bearing carries a dead vertical load resultant of $42 \times 10^6 \text{ N}$ rotating with a velocity of 0.033 rad/min. By floating the walls, the bearing is increasingly subjected to oscillations implied by wind and a pounding water stream, with a maximum resultant horizontal force of $350 \times 10^6 \text{ N}$ under full hydraulic head. Rotation of the walls and deformation of the structure makes the ball sliding over the bottom and back chairs, transmitting respectively vertical and horizontal loads to the anchor block, which introduces them into the foundation. The ball however not only slides through rotation but it is eccentrically loaded by friction, causing additional friction moments and rolling. Therefore, the resulting force displaces and the location where loads are introduced on the chair structure is variable. Just after the storm surge a situation may occur with a so-called 'negative hydraulic head' (low water level on the sea side) and then a resultant force of $50 \times 10^6 \text{ N}$ moves onto the front bearing.

Table 1
FEM analysis of local contact situation for a polymer pad in the back and bottom chair structure

Design factor	Back-chair bearing	Bottom-chair bearing	Comments
Global contact pressure (MPa)	31	34	Considering full bearing area
Loading factor (–)	2.61	2.53	Depending on pad filling pattern
Factor difference in local stiffness (–)	1.22	1.23	Non-uniform contact pressure distribution over pad
Local deformation (mm)	2.70	2.80	Vertical indentation due to total contact pressure
Extra deformation (mm)	0.56	0.72	Imperfect geometrical tolerances on pad and hole
Total contact pressure (MPa)	147	163	Local working conditions for polymer pad
Frictional design value (–)	0.25	0.25	Global frictional torque implied on steel structure

1.2. Characteristics of the ball joint

The ball-joint was analysed by global FEM calculations concerning the steel structures and a local calculation of the polymer pads. The global behaviour includes the modification of curvature radii between convex and concave surfaces (influencing the roll and slip behaviour of the ball with different resultant force), the stiffness and thickness of the interface (polymer pads have higher thickness and lower stiffness than a lubricating film), the implications of higher friction (global design values increased from 0.15 for MoS₂ to 0.25 for polymer pads) on strength of the construction, the distribution of the pads over the sliding surfaces,... As present research focuses on the local strength and friction of one single polymer pad, only results of the local FEM calculations as performed by Solico B.V. are detailed in Table 1 for the bottom and back bearings. Loads on the front bearing are inferior. The input for contact pressures results from global analysis concerning a full bearing area, with each parameter contributing to locally higher stresses represented by an additional factor. The local bearing area of the pads depends on the filling grade over the chair structures and differences in local stiffness of the chair structures result from variations in section. The ‘real’ calculated forces cause a vertical indentation of the bearing elements, while geometrical tolerances allow for locally higher deformation influencing the load distribution on two neighbouring pads. The total contact pressures on each pad, calculated at 163 or 147 MPa depending on the position, are rather conservative as it is assumed that effects of stiffness variation, local deformation and geometrical tolerance coincidence at the same location. For present design load of 150 MPa, the retained polymer pads are under quasi-hydrostatic conditions, leading the compressive and shearing forces into the steel structure through the walls and the bottom of the machined holes.

Based on environmental concerns, strength, low friction and application possibilities, UHMWPE pads are preferentially chosen since it is known from small-scale testing that it shows appreciable low friction and excellent abrasional wear resistance among other engineering polymers [2]. Its high toughness prevents fracture and the improved creep resistance compared to polyethylene reduces cold flow. UHMWPE has therefore been used successfully for over 35 years in common tribotechnics as bearing material in total

joint replacement components. Common contact stresses applied in tribological tests on UHMWPE are however within the range of 10–20 MPa, according to the situation occurring in hip or knee implants. Although, Collier et al. [3] found that the contact stresses in several non-conforming designs are much larger than the tensile yield strength of the polymer and rise towards the 30–40 MPa range with 80% of the total contact area that is typically overloaded above the 10 MPa damage threshold/fatigue strength. Collier and co-workers [3] cited a 21 MPa tensile yield strength for polyethylene, while Buechel et al. [4] used a 32 MPa compressive yield strength and a damage threshold of 5 MPa. Bartel et al. [5] used a 12.7 MPa yield strength, while Hayes et al. [6] used 14–15 MPa. High contact stresses are most often considered as responsible for surface damage with the evolution of a plasticity-induced surface layer as a precursor for wear. The best current solution towards reducing surface delamination and deformation lies in design optimisation of the contact stress distribution and minimisation of the deleteriously loaded area by maximising the bearing contact area. Presently a carbon/epoxy composite reinforcing ring is incorporated into a hybrid UHMWPE pad to ensure dimensional stability, allowing for sliding tests above the material’s yield strength. A simulation of the contact stress distribution on a hybrid UHMWPE pad within a machined hole is shown in Fig. 2.

An international test program at Ghent University (Laboratory Soete) and Stuttgart University (Materialprüfungsanstalt) was performed in parallel to the design process for evaluating static and dynamic friction on large-scale test samples in combination with creep under various preloads and different geometrical scales, giving additional insight into the reproducibility of the test results. The wear of polymer pads and counterfaces was evaluated by microscopic observations. The final concept was implemented and proven on-the-field by the Nederlandse Rijkswaterstaat.

2. Experimental

2.1. Test materials

A hybrid UHMWPE pad is schematically shown in Fig. 3 (scale 1:1), with a reinforcing carbon ring and a polymer lip

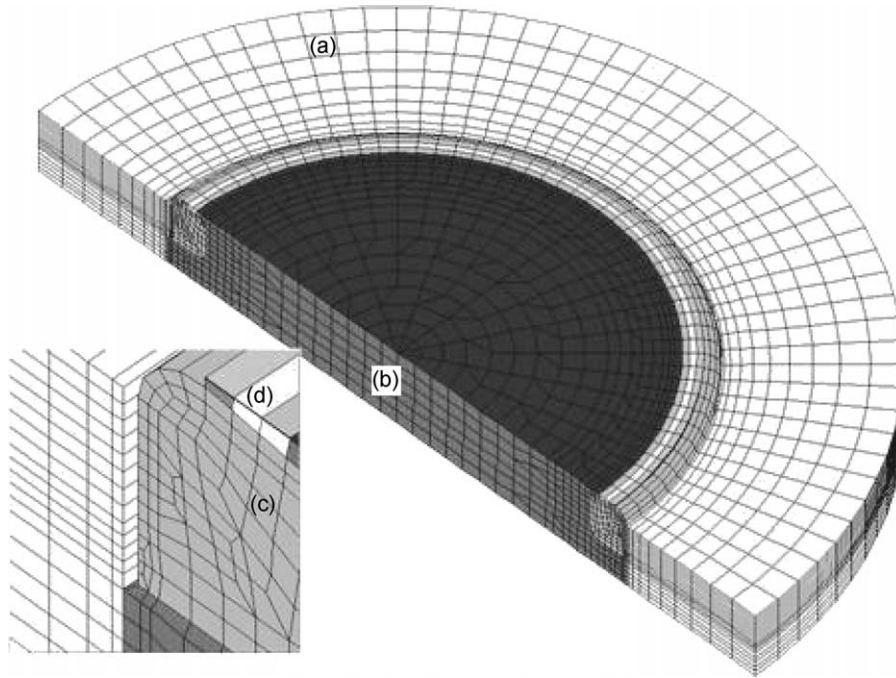


Fig. 2. FEM stresses on a UHMWPE polymer disc ($\text{\O} 249 \text{ mm} \times 40 \text{ mm}$) retained into a machined hole, (a) steel structure, (b) UHMWPE pad, (c) retaining carbon/epoxy ring, (d) polymer lip.

protecting the carbon ring against counterface contact under sliding. GUR 4120 is used as compression moulded UHMWPE with intrinsic viscosity 2100 ml/g , density 0.93 g/cm^3 , average molecular weight of $5 \times 10^6 \text{ g/mol}$ and mechanical properties given in Table 2 [7]. At low mechanical stress levels, the material can be used at temperatures in the region of $80\text{--}100 \text{ }^\circ\text{C}$ without substantial deformation. General pv -values of 0.06 MPa m/s are prescribed when used in unlubricated bearings with the maximum permissible surface pressure loading for bearings about 10 MPa , while present applied pv -value rises towards 0.75 MPa m/s under 150 MPa testing. The sliding surface contains a triangular pattern (side 13.5 mm) of circular undulations ($\text{\O} 4 \text{ mm}$) to hold an eventual lubricant. Patterned UHMWPE sliding surfaces have previously been used on lubricated small-scale test samples [8], leading to reduced friction and acting as a trap for wear debris that minimises third body wear. Therefore, Nishimura et al. [9] found reduced wear rates during pin-on-pad tests between patterned UHMWPE and stainless steel, although the lowering of wear under high loaded conditions seems not reproducible because the polyethylene surface plastically deforms. However, because polymers are compliant materials with relatively low tensile yield strength, an optimisation of the hole geometry with hole diameters and path to gap lengths should retain the favourable properties. The patterned surface presently should retain eventual dust or wear debris and therefore contributes to reduced ploughing components and protection of the counterface against wear. The rubber ring near the bottom ensures axial

fixation of the hybrid pad into its holder, especially when mounted into the back scale of the ball-joint. A hole with 2 mm diameter in the centre of the pad allows for evacuation of air from the holes during mounting. The reinforcing composite ring is made of unidirectional high-modulus carbon fiber Toray T700 12 K (1.8 g/cm^3) and epoxy resin (1.09 g/cm^3) that is wound on tubes and afterwards machined into separate rings. It has fiber percentages between 58 and 63% and porosity content $< 2.5\%$ needed for structural integrity.

Counterfaces measure $400 \text{ mm} \times 210 \text{ mm} \times 20 \text{ mm}$ and either consist of steel St 37–2 N ($\text{HB} = 140 \text{ N/mm}^2$, $R_e = 235 \text{ MPa}$, $R_m = 380 \text{ MPa}$) with roughness grooves perpendicular to the sliding direction ($R_a = 1.12 \text{ }\mu\text{m}$ and $R_t = 9.94 \text{ }\mu\text{m}$ parallel to the sliding direction), or a soft Zn-phosphate primer coating (alkyd-resin based, density 1.4 kg/l , $47 \text{ vol}\%$ solids) with $R_a = 1.29 \text{ }\mu\text{m}$ and $R_t = 9.18 \text{ }\mu\text{m}$ measured parallel to the sliding direction. The coating is required to protect against corrosion and is applied on a sand blasted steel St 37–2 N substrate with original roughness $R_a = 3.50 \text{ }\mu\text{m}$ in order to obtain good adhesion. Different application methods are investigated: brushed, sprayed and rolled. The average coating thickness in wet conditions is $175 \text{ }\mu\text{m}$ and $40\text{--}80 \text{ }\mu\text{m}$ in dry conditions (drying time 1 h , curing time 1 week). Although favourable for corrosion protection, its friction and wear performance under high loads should be verified. It is however noticed from other sliding tests on soft coatings performed by e.g. Benabdallah [10], that they are easily removed under high loads.

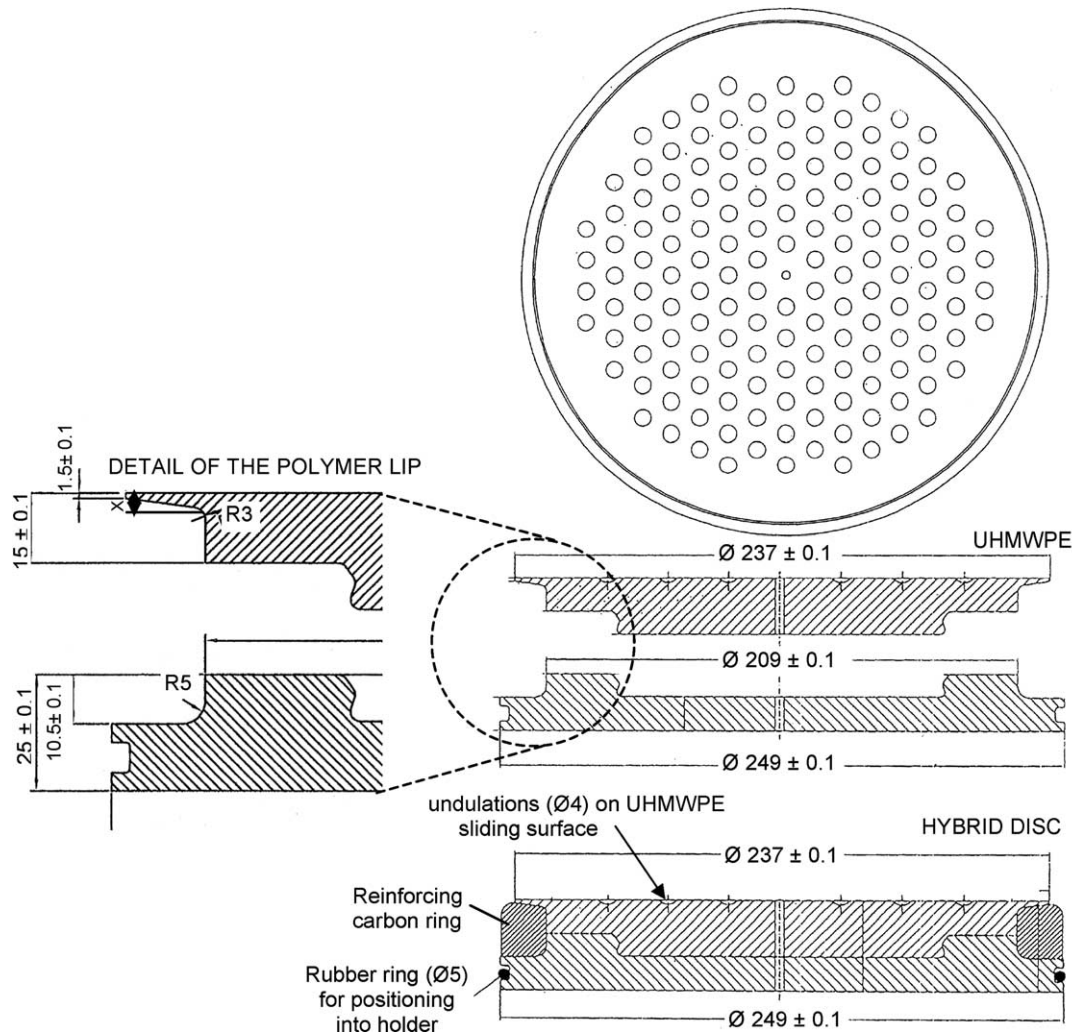


Fig. 3. Hybrid UHMWPE-discs with a carbon/epoxy composite reinforcing ring (scale 1:1, lengths and tolerances in mm).

2.2. Large-scale friction and wear testers

Two tribotesters at Ghent University (Fig. 4(a)) and Stuttgart University (Fig. 4(b)) are used with different loading capacities, allowing to include pads with diameter 60 mm (scale 1:4.2) and diameter 150 mm (scale 1:1.7) tested on Fig. 4(b) and pads with diameter 175 mm (scale 1:1.43) tested on Fig. 4(a). Both test equipments allow comparing inter-laboratorial reproducibility of the test results.

Large-scale verification tests on friction, wear and strength of a hybrid UHMWPE pad were performed on the tribotester shown in Fig. 4(a) (Ghent University),

applying horizontal shear forces under normal loads between 15 and 150 MPa. Two friction pairs are tested at once, each consisting of a polymer pad and an uncoated or coated steel counterface, placed on top and on bottom of the test machine. The polymer pads are fixed in circular holders in the frame of the tribotester, supported by leaf springs that provide high stiffness to resist the horizontal sliding forces. The central sliding bloc contains two counterface plates on top and on bottom and provides a reciprocating motion through the horizontal jacks on the left (F_l) and the right (F_r). With a single sliding stroke of 240 mm, the total sliding distance comprises 10 sliding cycles (one cycle is a double stroke) or 4.8 m for each normal load. The sliding

Table 2
UHMWPE hybrid pad mechanical and thermal properties [7]

	Tensile modulus (MPa)	Yield stress (MPa)	Elongation at yield (%)	Elongation at break (%)	Tensile creep stress (MPa)	Vicat softening point (°C)	Melting temperature (°C)
UHMWPE	720	>17	<20	>50	460 (1 h, 0.5%), 230 (1000 h, 0.5%)	80	130

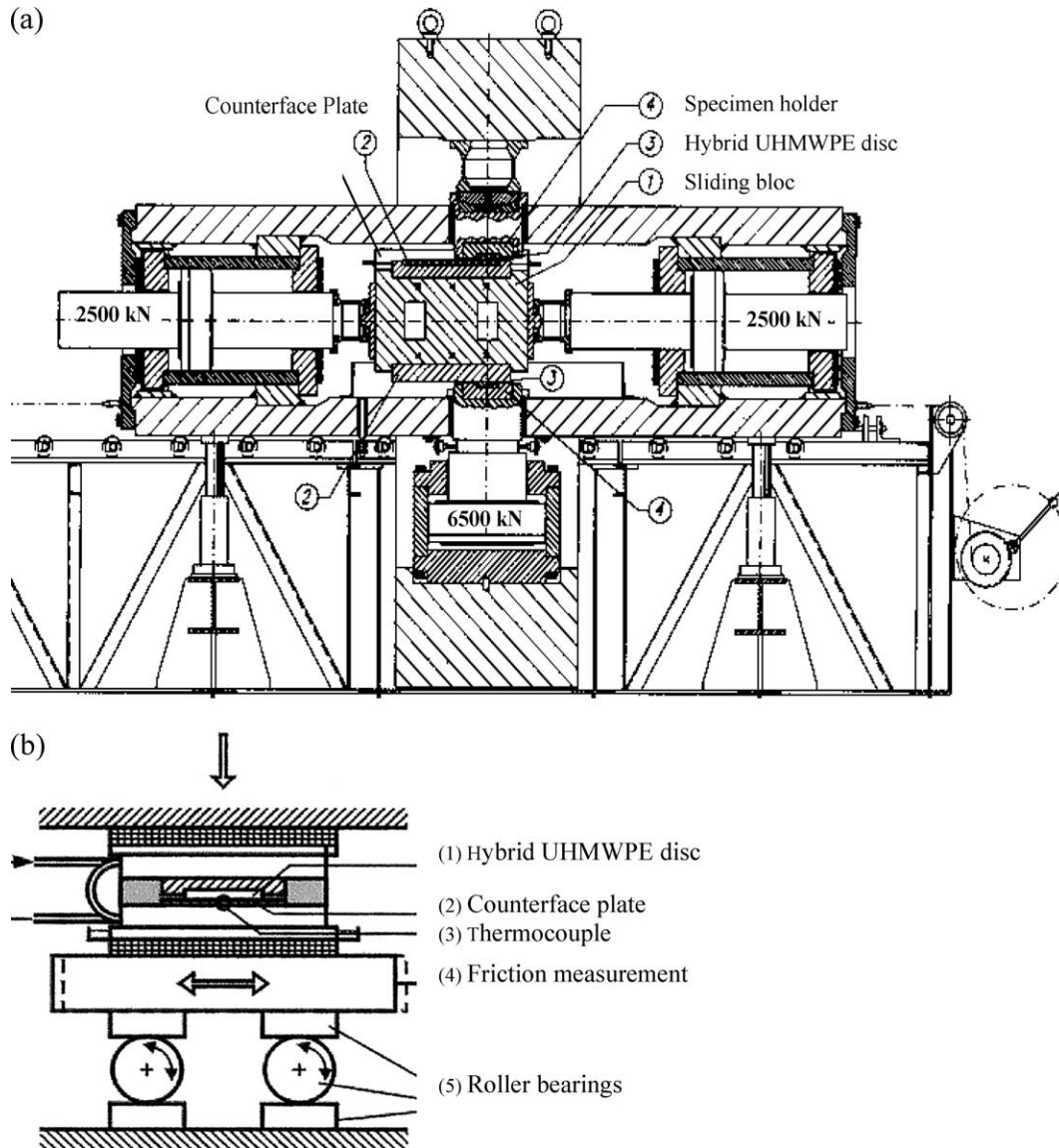


Fig. 4. Large-scale test equipment at (a) Ghent University, (b) Stuttgart University.

velocity is constant at 5 mm/s over mostly the total sliding stroke, controlled by the hydraulic circuit. The normal load (F_n) is applied by a jack placed in the vertical column, providing contact between the polymer test specimen and their respective steel counterfaces. Coefficients of friction are calculated according to $\mu = 1/2|(F_1 - F_r)/F_n|$ representing an average value between two friction couples. Sliding temperatures are continuously measured by a *K*-type thermocouple, positioned at 20 mm beneath the contact surface (i.e. at the interface of the steel counterface and the central sliding bloc). The initial counterface temperature is 15 °C, obtained by internal cooling of the central sliding bloc by water flow.

Fig. 4(b) (Stuttgart University) presents an alternative test rig that has been used for detailed characterisation of the running-in sliding process, investigating the effect of static preloads and creep on the initial static coefficient

of friction and variations in friction after intermediate wear paths. The static and dynamic friction forces can be measured very accurately since the actuator is driven by a spindle and the roller bearings have very low and calibrated friction. As the maximum load capacity is lower than the Ghent University tribotester, test are mainly performed under 15 MPa, where the highest friction is expected to occur. Literature models [11] however predict lower coefficients of friction under increasing normal loads, as should be verified on the Ghent University tribotester. Pads of smaller diameter were tested when verification of running-in at higher contact pressures is necessary, however results should be carefully checked with the full-scale tests due to geometrical shape factors possibly contributing to higher friction. Nevertheless, as only one test specimen is incorporated, measurements of static friction should be more accurate.

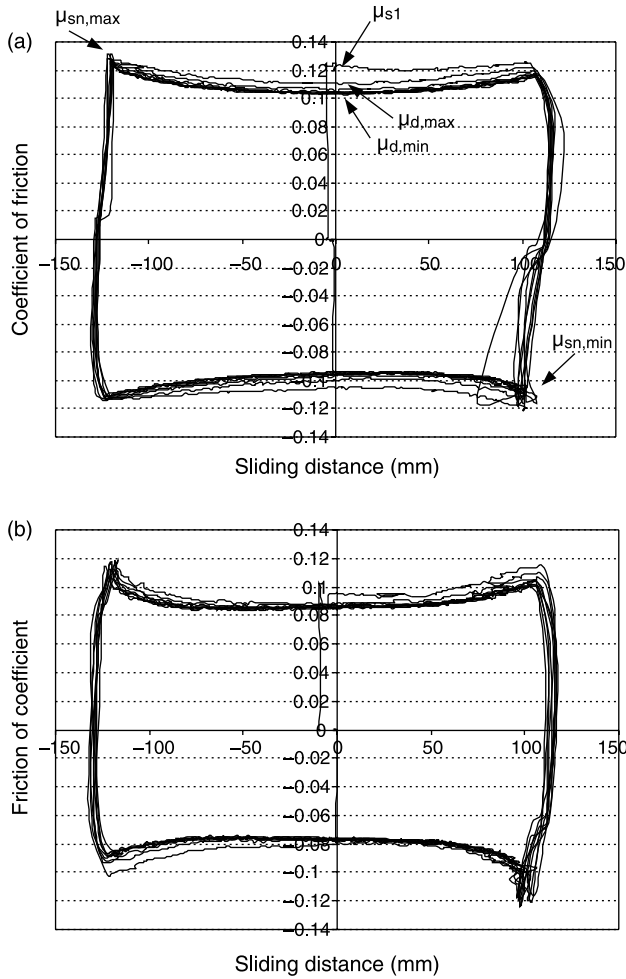


Fig. 5. Friction-displacement characteristic for a hybrid UHMWPE-disc sliding against (a) steel and (b) Zn-phosphate coating under 15 MPa, with indication of static and dynamic friction values.

3. Test results, calculations and observations

Both selection and verification tests are presented, done to explore suitable material combinations and to evaluate its performance in the storm surge barrier. Besides the dynamic tests presently discussed, also large-scale static tests were performed, detailed in Ref. [12]. Friction curves are recorded as a function of the reciprocating sliding motion

as shown in Fig. 5, with an indication of the characteristic friction values for both static friction (μ_{s1} at the start or $\mu_{sn,min}$ and $\mu_{sn,max}$ at reversal of the sliding motion) and dynamic sliding ($\mu_{d,min}$ and $\mu_{d,max}$ in the centre of the sliding stroke).

3.1. Effects of counterface type on friction and wear of hybrid pads (tribotester in Fig. 4(a) used)

3.1.1. Friction

Test results in Table 3 show the coefficients of friction in sliding of a hybrid UHMWPE pad (Ø 175 mm) against steel and a sprayed Zn-phosphate coating under different contact pressures, without static preloading. Steel surfaces are included in the test program as polymer/steel contact possibly occurs after the coating has worn. The initial static friction μ_{s1} is higher than static friction at subsequent reversals of the sliding direction, own to the original steel or coating roughness and application method of the Zn-phosphate coating (Table 4). The evolution of friction with sliding distance is shown in Fig. 6(a), revealing that friction stabilizes less frequently on Zn-phosphate coatings compared to steel, mainly under low contact pressures (15–30 MPa): friction is constant after 0.7 m sliding against steel and progressively decreases against Zn-phosphate coating, where even after 2 m sliding distance friction still lowers. This observation is related to progressive smoothening of the soft coating as shown later. The effect of different coating application methods on friction (Table 4) illustrates that it has minor influences on the steady-state dynamic friction, although brushed or sprayed and polished coatings provide lower static friction than rolled coatings. Differences between friction measured in Tables 3 and 4 are attributed to a preload of 50 MPa prior to sliding for the latter tests. For the rolled coating, mainly the static coefficient of friction (μ_{s1} and μ_{sn}) rises towards 0.22 under 15 MPa, possibly due to different initial coating roughness. After several sliding cycles, the soft Zn-phosphate coating becomes smoothened, providing nearly identical friction conditions for the different application methods. Sprayed coatings with controllable thickness are finally preferred for the ball protection: the coating thickness ranges between 37 and 66 μm with average

Table 3
Effect of counterface type on large-scale friction of hybrid UHMWPE pads

p (MPa)	Steel counterface					Zn-coated counterface				
	Static			Dynamic		Static			Dynamic	
	μ_{s1}	$\mu_{sn,min}$	$\mu_{sn,max}$	$\mu_{d,min}$	$\mu_{d,max}$	μ_{s1}	$\mu_{sn,min}$	$\mu_{sn,max}$	$\mu_{d,min}$	$\mu_{d,max}$
15	0.12	0.11	0.12	0.10	0.11	0.10	0.11	0.12	0.08	0.09
30	0.10	0.10	0.11	0.09	0.10	0.10	0.08	0.09	0.07	0.08
60	0.08	0.07	0.08	0.06	0.07	0.05	0.06	0.07	0.04	0.04
90	0.06	0.05	0.06	0.05	0.05	0.04	0.05	0.05	0.03(5)	0.03(5)
120	0.05	0.05	0.05	0.04	0.04	0.03(5)	0.04	0.04	0.03	0.03
150	0.04	0.04	0.04	0.03(5)	0.03(5)	0.03	0.02(5)	0.03	0.02(5)	0.02(5)

Table 4
Influence of application method of Zn-phosphate coating and contact pressure on friction

Application method of Zn-phosphate primer coating	Contact pressure (MPa)	Static			Dynamic	
		μ_{s1}	$\mu_{sn,min}$	$\mu_{sn,min}$	$\mu_{d,min}$	$\mu_{d,max}$
Brushed	15	0.19	0.10	0.10	0.07	0.08
	30	–	0.07	0.08	0.04	0.05
	90	–	0.03	0.04	0.02	0.02
	175	–	0.02	0.03	0.02	0.02
Rolled	15	0.22	0.13	0.14	0.09	0.10
	30	–	0.08	0.09	0.06	0.06
	90	–	0.04	0.05	0.03	0.03
	175	–	0.03	0.04	0.03	0.03
Rolled and polished	15	0.20	0.12	0.12	0.09	0.10
	30	–	0.08	0.10	0.06	0.06
	90	–	0.04	0.05	0.03	0.04
	175	–	0.03	0.04	0.03	0.04
Sprayed	15	0.21	0.10	0.10	0.06	0.07
	30	–	0.06	0.08	0.04	0.05
	90	–	0.03	0.04	0.02	0.02
	175	–	0.02	0.03	0.02	0.02
Sprayed and polished	15	0.18	0.10	0.11	0.07	0.08
	30	–	0.06	0.08	0.04	0.05
	90	–	0.05	0.06	0.03	0.03
	175	–	0.02	0.03	0.02	0.02

thickness of 51 μm after complete curing. In relation to the contact pressures, a strong decrease in friction coefficients for higher contact pressure is found (Fig. 6(b)). Uetz and Hakenjos [13] give a relationship for UHMWPE sliding against austenitic stainless steel as $\mu = Cp^{-n}$ with $n = 0.23$. Present results fit a power law with $n = 0.46$ for $\mu_{s,min}$ and $n = 0.58$ for $\mu_{d,min}$ ($R^2 = 0.97\text{--}0.99$) in contact with steel, while $n = 0.47$ for $\mu_{s,min}$ and $n = 0.52$ for $\mu_{d,min}$ ($R^2 = 0.92\text{--}0.97$) for Zn-phosphate coated steel. These exponents imply the influence of huge plastic deformation at the contact asperities with a change from partial contact towards full contact under high loads, as referred to on micro-scale by Pascoe et al. [14]. It seems that friction for contact pressures above the polymer's yield strength is much lower than

traditional low-load applications, implying coefficients of friction for UHMWPE around 0.2–0.3 [15].

3.1.2. Wear and deformation

A macroscopic photograph of the hybrid UHMWPE-pad before and after sliding against a Zn-phosphate coating under 30 and 150 MPa is shown in Fig. 7. The UHMWPE sliding surface is examined by optical microscopy in Fig. 8 after sliding against steel and a Zn-phosphate coating. It has been observed that direct contact between the reinforcing carbon ring and the counterface or loose of carbon fibers in the sliding interface leads to unacceptable counterface wear [12]. Therefore, a polymer lip is designed as such that it flows over the carbon ring during the initial loading step or

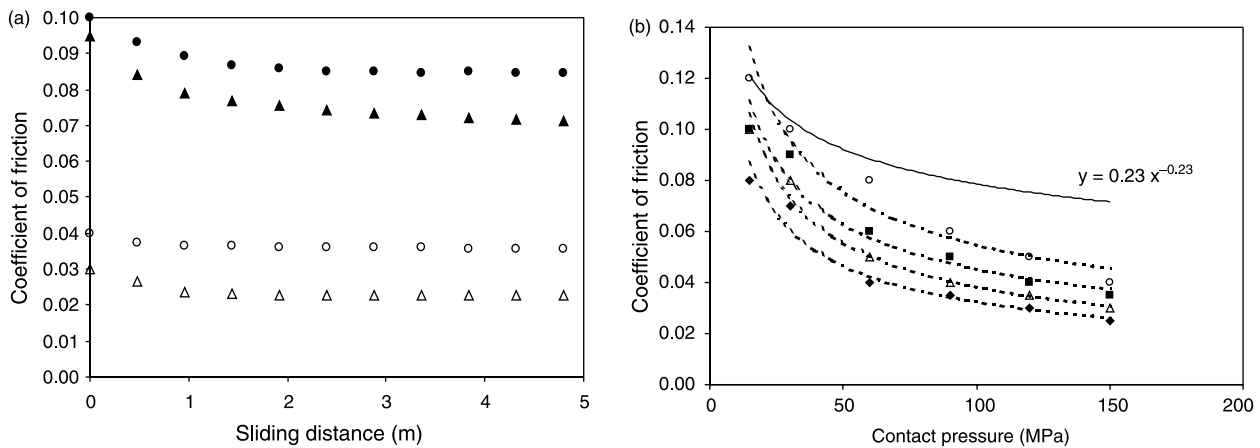


Fig. 6. Evolution of running-in friction with sliding distance and contact pressure, (a) sliding distance: ● UHMWPE/steel 30 MPa, ▲ UHMWPE/coating 30 MPa, ○ UHMWPE/steel 150 MPa, △ UHMWPE/coating 150 MPa, (b) contact pressure: ○ μ_{s1} /steel ($y = 0.46x^{-0.46}$) ■ $\mu_{d,min}$ /steel ($y = 0.40x^{-0.47}$) △ μ_{s1} /coating ($y = 0.56x^{-0.53}$) ◆ $\mu_{d,min}$ /coating ($y = 0.35x^{-0.52}$).

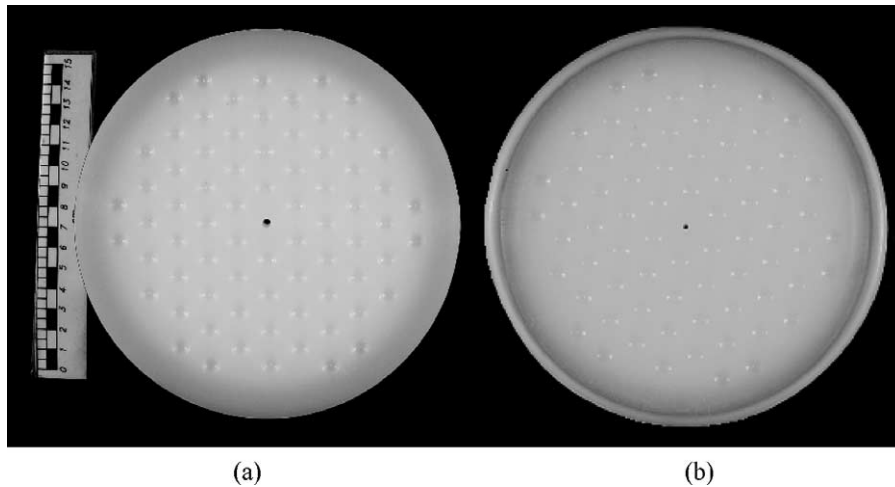


Fig. 7. Macroscopic photograph of a hybrid polymer disc (diameter 175 mm) (a) before and (b) after sliding under 150 MPa against Zn-phosphate coating.

during the first sliding cycle, protecting the counterface against abrasive wear. In present case, the cold-flow of UHMWPE is favourably used, referring to a surface phenomenon that is due to deformation of the material under shear forces in absence of elevated temperatures [16]. The flow of different lip geometries was experimentally evaluated under static and dynamic load, with diameters and thicknesses at the onset of the lip important factors, as detailed in Fig. 3. Curling of the lip should be avoided, causing friction instabilities during running-in. This lead to

the reduction of the original lip diameter from 244 ± 0.1 mm towards finally 237 ± 0.1 mm. Sliding tests on pads with different lip thicknesses (the value 'X' refers to the lip thicknesses as defined in Fig. 3) provided identical friction coefficients, although differences in deformation are shown in Table 5. An extrapolated lip thickness X between 4.2 and 5.0 mm is finally applied, as smaller thickness cause instable curling. The increase in average lip diameter by permanent flow after static loading (150 MPa) then is 2%, after sliding it is 0.3% at 30 MPa and 4% at 150 MPa.

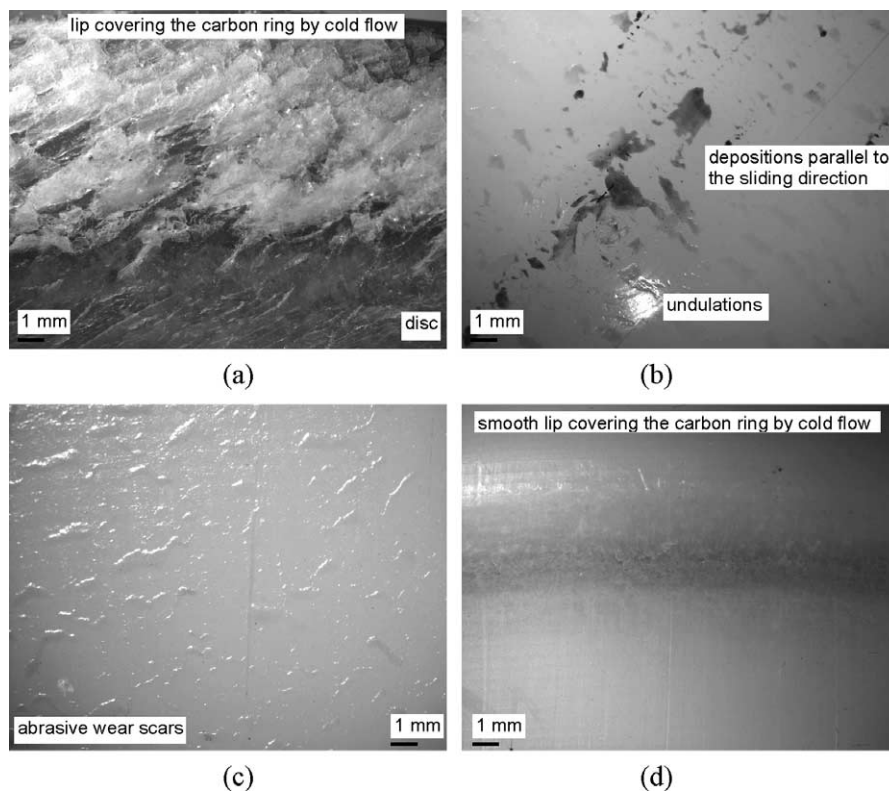


Fig. 8. Microscopy of the UHMWPE surface after sliding under 150 MPa against (a), (b), (c) steel, leading to abrasive wear and (d) Zn-coating, remaining smooth.

Table 5
Dimensional changes of a hybrid UHMWPE pad after sliding under 30 and 150 MPa, for different lip thicknesses 'X' as defined in Fig. 3

	Original lip thickness X (mm)	Thickness of pad (mm)	Diameter pad near bottom (mm)	Diameter of polymer lip on top (mm)	Diameter carbon ring (mm)
Before sliding	4.2	40.30	174.61	169.65	171.20
After sliding (30 MPa)		40.22	174.72	170.10	171.20
After sliding (150 MPa)		40.50	174.81	177.06	171.20
Before sliding	5.0	40.18	174.60	169.83	171.34
After sliding (30 MPa)		40.05	174.65	170.18	171.34
After sliding (150 MPa)		40.15	174.79	175.60	172.34
Before sliding	4.0	40.33	174.69	169.67	171.18
After sliding (30 MPa)		40.05	174.70	170.03	171.19
After sliding (150 MPa)		Lip curling	Lip curling	Lip curling	171.19

Deformation of the UHMWPE hybrid pad after a 30 and 150 MPa sliding test against a Zn-primer coating (Table 5) reveals extreme dimensional stability of the carbon reinforcing ring with slight decrease in thickness after 30 MPa due to visco-elastic indentation and increase in thickness after 150 MPa due to lip formation. Also the dimensional tolerances between the pad and hole diameter seems important, as the diameter of the pad near the bottom permanently increases by plastic flow into the sample holder. Changes in lip diameter reveal partial covering of the carbon ring after 30 MPa and full covering after 150 MPa. After sliding against steel the lip becomes too thin and it suffers abrasive wear seen as shearing bands in Fig. 8(a). These irregular shapes contribute to high friction in sliding against steel, as seen in Table 3. The surface undulations remain undeformed after sliding (Fig. 8(b)) and some depositions of degraded wear debris are observed on the polymer surface. It seems however that wear debris is not preferentially deposited into the undulations, but they rather form discontinuous bands parallel to the sliding direction. One hypothesis is that the undulations visco-elastically deform under high loads, not acting as a trap for wear debris, and recover after unloading as observed under static loading tests. Moreover, abrasive wear scars (Fig. 8(c)) were observed after sliding against steel, more prominently manifesting for a wear test on atmospherically aged UHMWPE. However, these were not observed after sliding against a Zn-primer coating (Fig. 8(d)) and should not occur on the in situ ball-joint, as the sliding surfaces function under entirely controlled atmosphere. After sliding against the Zn-phosphate coating, the UHMWPE surface and lip remain smooth in accordance with the reported low and stable friction.

The aspect and surface roughness profiles of the steel and Zn-phosphate coated counterfaces after sliding are evaluated in Figs. 9 and 10, respectively. The counterface roughness profiles are measured before and after large-scale sliding, both parallel (//) and/or perpendicular (\perp) to the sliding direction, with characteristics R_a and R_t as given in Table 6.

- In case of sliding against steel wear debris is observed on the sliding counterface, that accumulates at the borders of

the sliding zone, consisting of white (UHMWPE) and black (degraded UHMWPE and/or carbon) particles detached from the polymer lip. The wear debris deposited into the machined grooves causes a very slight decrease in steel roughness and hardly noticeable changes in surface profile at 60 and 150 MPa. After the surface is rinsed with acetone the counterface roughness increases again to nearly its initial value, indicating that the steel surface not has been worn.

- In sliding contact with the soft Zn-phosphate coating, no UHMWPE wear debris is observed. The aspect of the coating has changed from coarse grained (mat grey colour) to fine grained (glossy grey colour) after sliding. From the roughness profiles at 150 MPa it is concluded that the local roughness peaks have flattened, while the waviness still remains. There is a general decrease in surface roughness after sliding, although some wear grooves parallel to the sliding direction result in a roughness $R_{a\perp}$ that is somewhat higher compared to $R_{a//}$. A macroscopic view on the slid coating area reveals some prints of the pad undulations together with few slip-marks at the reversals of the sliding motion. The latter are an indication of slight stick-slip (mainly at 15–30 MPa) at the reversals of the sliding stroke, as indicated by reasonably high $\mu_{s,n}$ in Fig. 5(b). Contact between carbon fibers from the reinforcing ring and the coating should however be avoided, since they cause slight cracks and wear marks as microscopically shown after sliding under 30 MPa, when the carbon ring was not yet fully covered. However, they do not affect the adhesion of the coating to the substrate nor the corrosion resistance nor the beneficial sliding properties of the coating layer after high load sliding. On the contrary, it was visually observed that the cracks disappeared after 150 MPa sliding showing that the coating seems to have limited self-repairing capability, due to local plastification as evaluated in paragraph 3.2. Further research on the nature of those cracks and eventual relations to the coating drying time was not done, although it was noticed from static load tests reported in Ref. [12] that higher curing times result in better coating adhesion.

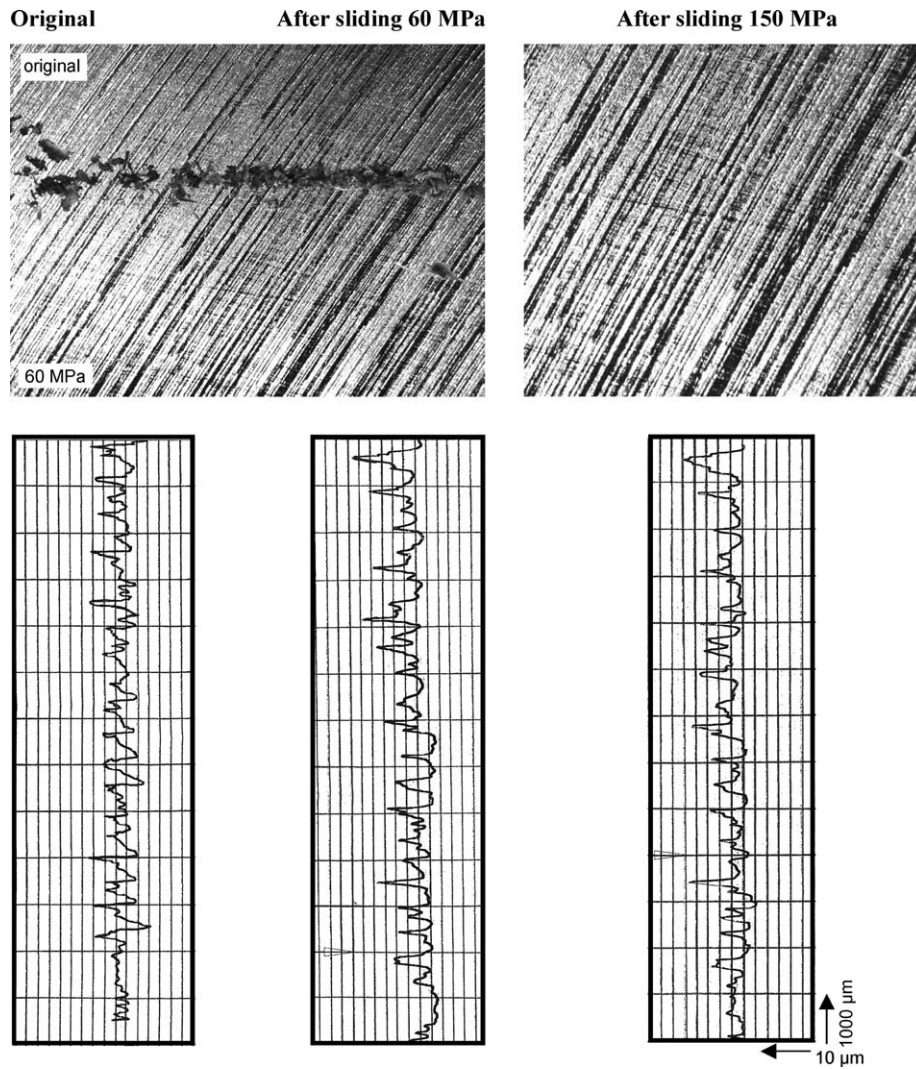


Fig. 9. Evaluation of steel surface before and after sliding under 60 and 150 MPa.

- On both steel and Zn-coated counterfaces, no polymer transfer nor film formation could be visually observed.

3.2. Evaluation of the sliding temperature (tribotester in Fig. 4(a) used)

From dynamic friction and contact pressures, the bulk- and flashtemperatures are theoretically calculated according to models of Blok and Archard [17], specifically developed for circular contact geometries, and compared to experimental values in Table 7. Tribological test results are considered from Table 3. For a uniform distribution of the heat flow over the contact area, the steady-state temperature rise at the centre of the contact is given by Eq. (1), for a heat intensity $q = \mu p v$ (W/m^2), contact diameter $2\ell = 175$ mm and thermal conductivity $k = 33$ W/mK. The generated heat flow is however concentrated at the surface asperities of both contact bodies, resulting in a local flashtemperature calculated from Eq. (2), taking into account the thermal

diffusivity $a = 9.09 \times 10^{-6}$ m²/s.

$$T_{\text{bulk}} = \frac{q\ell}{k} = \frac{\mu p v \ell}{k} \quad (1)$$

$$T_{\text{flash}} = 1.14 \frac{\sqrt{\ell a v}}{k} \mu p \quad (2)$$

The bulktemperatures are experimentally measured at 20 mm beneath the sliding interface, and are therefore corrected by a linear conductive law with $\Delta T = qs/k = \mu p v s/k$ for a measuring depth $s = 20$ mm, estimating the bulk temperature at the sliding interface. It seems that experimental measurements of interface temperatures remain below the theoretical bulk temperatures, possibly due to convection effects not taken into account and/or the extremely low sliding velocities allowing for intermediate cooling of the sliding surfaces. Also complete temperature stabilisation was not attained during tests with short sliding distances. However, it reveals that both the experimental and the calculated bulktemperatures are below the softening

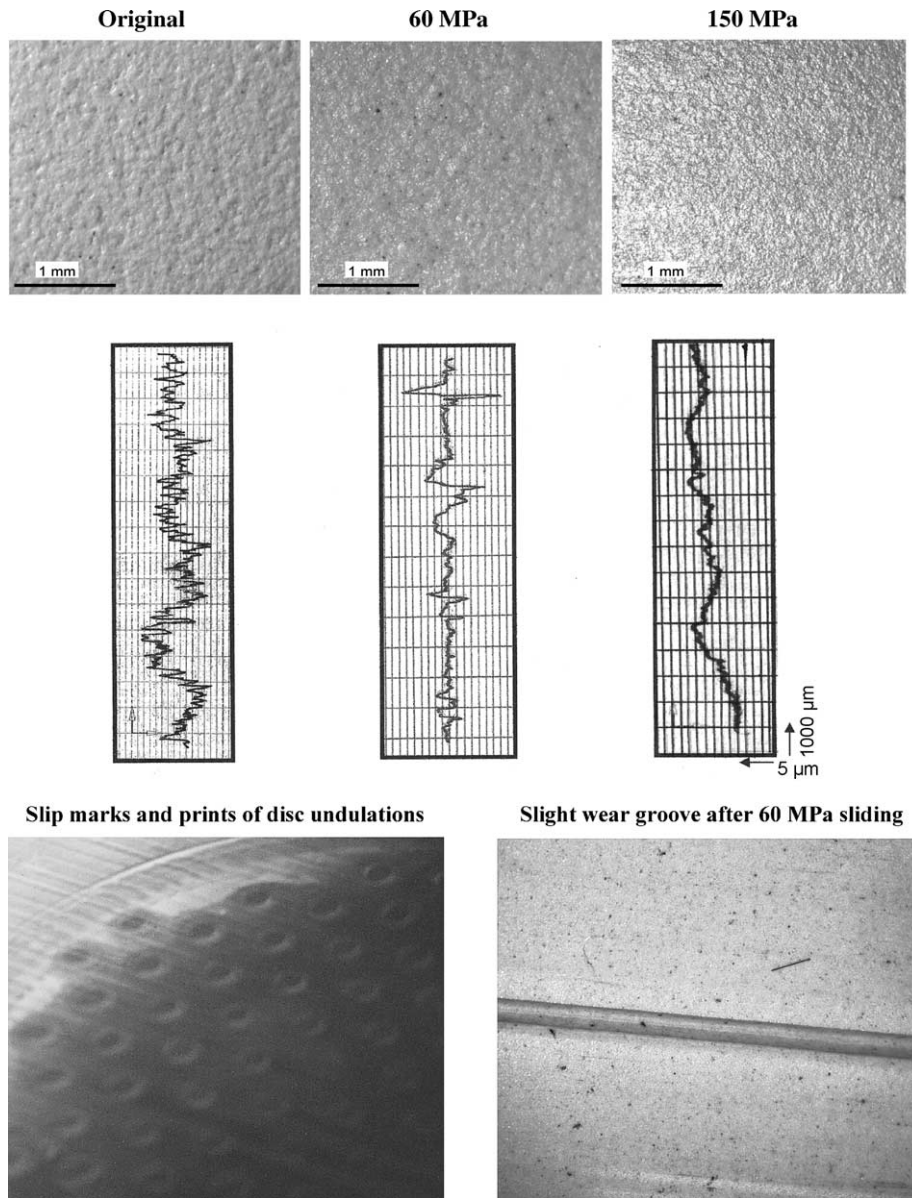


Fig. 10. Evaluation of Zn-phosphate coated counterface and roughness profile.

point of 80 °C (ISO 306) for UHMWPE [7], and that the local flash temperatures are below the melting point of 130 °C (ISO 3146). The latter flash temperatures only govern over approximately 10 μm beneath the contact surface, not influencing the bulk material properties. As creep is

however mainly determined by the bulk properties, it seems that high normal loads exceeding the material's yield strength are more important than frictional heating for causing an increase in lip diameter. Moreover, also static (isothermal) tests were performed at 23 °C to simulate the

Table 6
Steel and Zn-coated counterface roughness before and after large-scale sliding

p (MPa)	Steel counterface						Zn-coated counterface							
	Original		With depositions		Without depositions		Original				After sliding			
	$R_a \perp$	$R_t \perp$	$R_a \perp$	$R_t \perp$	$R_a \perp$	$R_t \perp$	$R_a //$	$R_t //$	$R_a \perp$	$R_t \perp$	$R_a //$	$R_t //$	$R_a \perp$	$R_t \perp$
60	1.21	11.86	1.08	10.62	1.14	10.61	1.29	9.18	1.35	9.30	0.45	4.20	0.83	6.43
150	1.14	10.61	1.10	10.69	1.19	11.12	0.45	4.20	0.83	6.43	0.29	2.86	0.44	4.30

Table 7

Evaluation of experimental and corrected bulktemperatures compared to calculated bulk- and flashtemperatures, according to Blok and Archard [17] for UHMWPE pads sliding against a Zn-phosphate coating (initial temperature 15 °C)

Contact pressure (MPa)	Experimental bulktemperatures (°C)		Interface temperature	Calculated temperatures (°C)	
	Measured	Correction ΔT		T_{bulk}	T_{flash}
15	20	4	24	33	56
30	23	7	30	46	89
60	27	7	35	46	89
90	28	10	38	56	112
120	30	11	41	62	120
150	32	12	44	65	125

increase in lipdiameter by cold-flow. For sliding tests, local flashtemperatures exceeding the material's softening point however contribute to the low friction observed under high normal loads, as the yield stress progressively drops from 17 MPa at 20 °C to 5 MPa under 120 °C by softening. The lack of surface melting is in accordance with the absence of a polymer transfer film. Considering the Zn-phosphate coating, it reveals however that temperatures in high-load sliding tests locally exceed the thermal coating stability (120 °C), leading to plastification that is favourable for smoothing of local cracks and the self-repairing capability as earlier mentioned.

3.3. Effects of static preload on friction of hybrid pads (tribotester in Fig. 4(b) used)

Verification tests on a hybrid UHMWPE-pad/Zn-phosphate primer coating combination were performed, closely related to the practical functionality in the ball-joint. During a periodic standstill before functioning of the ball-joint, a static contact between the UHMWPE hybrid pad and the Zn-phosphate primer results in creep and/or it enhances the adhesion between the polymer pad and the coating. The influence on static and dynamic friction of a short time preload applied before sliding is therefore investigated. Firstly, the static load bearing capacity of a

full-scale pad (\varnothing 250 mm) is evaluated on a vertical hydraulic press, recording the stress-strain characteristics and creep deformation. The pads were loaded a 30 MPa/min with each of the loading steps 30, 60, 90, 120 and 150 MPa remaining constant during 2 h (Fig. 11(a)). Finally, the creep at working conditions of 150 MPa was investigated during 24 h constant loading (Fig. 11(b)). Short-time overload conditions at 200 MPa (3 h) and 400 MPa (1 h) did not affect the integrity of the hybrid pads. With the hybrid pads positioned into their retaining holes, a loading capacity of 400 MPa is guaranteed, with gradual increasing stiffness at higher loads because of the expansion and clamping of the pad into its holder.

Table 8 gives the coefficients of friction for sliding tests on hybrid pads that are previously subjected to a static preload of 50 or 75 MPa. The pads are mounted in a backing plate with a recess of appropriate diameter (identical as the ball-joint, described in Fig. 1) and covered with a Zn-coated counterface. A first series of pads (\varnothing 60 mm) is 16 h preloaded at 50 MPa and a second series of pads (\varnothing 150 mm) is 16 h preloaded at 75 MPa. Afterwards the test specimens are transferred to the tribotester under fixed conditions for a sliding test under different normal loads. The initial value of friction μ_{s1} at 15 MPa is significantly higher than previous sliding tests from Table 2, while the dynamic friction

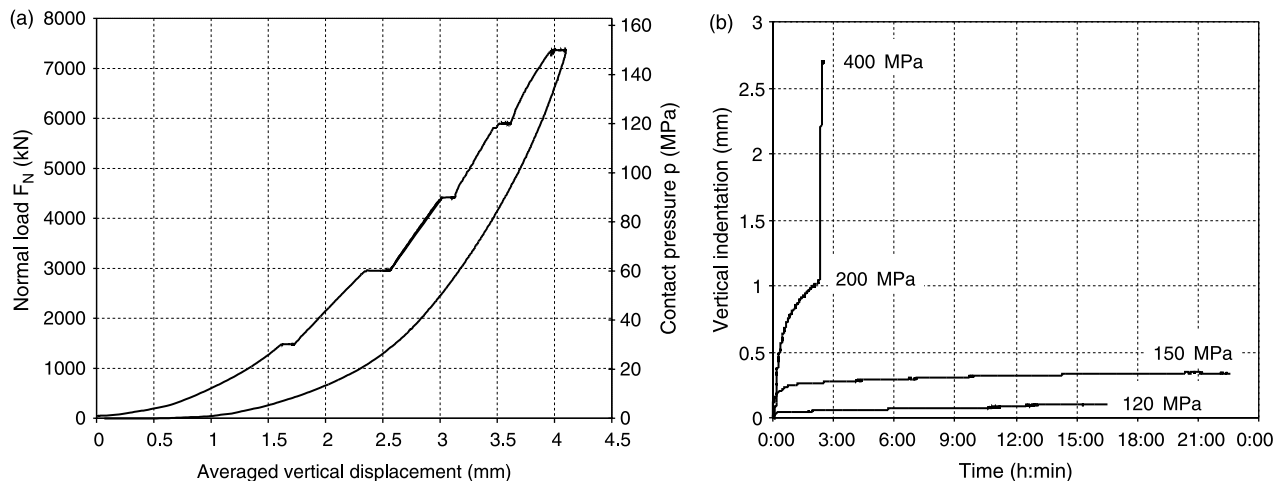


Fig. 11. Static loading capacity and vertical indentation as a function of (a) load, (b) time.

Table 8
Effect of preload on large-scale friction of hybrid UHMWPE pads

p (MPa)	50 MPa preload against Zn-coated steel					75 MPa preload against Zn-coated steel				
	Static			Dynamic		Static			Dynamic	
	μ_{s1}	$\mu_{sn,min}$	$\mu_{sn,max}$	$\mu_{d,min}$	$\mu_{d,max}$	μ_{s1}	$\mu_{sn,min}$	$\mu_{sn,max}$	$\mu_{d,min}$	$\mu_{d,max}$
15	0.21	0.10	0.10	0.06	0.07	0.14	0.08	0.09	0.05	0.06
30	–	0.06	0.08	0.04	0.05	0.06	0.05	0.05	0.03	0.04
90	–	0.03	0.04	0.02	0.02	–	–	–	–	–
150	–	0.02	0.03	0.02	0.02	–	–	–	–	–

is presently lower after a preload is applied. A high friction at start μ_{s1} is attributed to bonding of the polymer sliding surface to the soft Zn-coated counterface by plastic deformation, while a lower dynamic friction either results from compaction and orientation of the crystalline lamellae structure of polyethylene or from the height reduction of the surface asperities by creep [18].

3.4. Effect of intermediate wear paths on friction and wear of hybrid pads (tribotester in Fig. 4(b) used)

The functioning of a ball-joint during closure or retaining a storm implies multidirectional movements of the sliding surfaces. The final design aims a total wear path of 300 m for the ball over the pads without constrictions of wear on the sliding properties, implying that the storm surge should function for 5 years without additional maintenance. The total sliding distance is calculated from the rotations of the joint during one test closure every year and one closure for a two-hydraulic head storm as a simulation for maximum wear. Therefore, the influence of three subsequent wear paths (100 m each, under 75 MPa) perpendicular to the motion of the friction test is experimentally investigated in Fig. 12, revealing a gradual increase in both static and dynamic friction with ongoing sliding. The effect of a cross-path motion on wear of UHMWPE was previously described by Turell et al. [19] for small-scale samples and is explained by orientation of the molecular chains at the sliding surface. Previous studies showed that motion in the perpendicular sliding leads to plastic deformation and molecular orientation, whereas motion in the sliding test direction leads to material removal by intermolecular splitting. Present large-scale tests however not revealed excess wear compared to single reciprocating motion. Multi-directional motions were simulated on small-scale by e.g. Wang et al. [20] and explained by the energy dissipation in each of the sliding directions. Under present test conditions, the aspect ratio of the cross-shear motion seems large enough to evoke differences in friction. If molecules are allowed to align perpendicular to the friction motion during an intermediate wear path of 100 m, they cause higher resistance in the friction test, although still remaining below present design value.

4. Discussion and design verification

It is demonstrated that friction of a hybrid UHMWPE-pad/Zn-phosphate coating is low and test results obtained on different large-scale tribotesters with different geometric scales are reproducible. A modelling factor $\gamma_m = 1.25$ has been applied on experimental friction coefficients for compensating statistical deviation in test results. For determination of the design coefficient of friction from experimental results, both the global and local stress

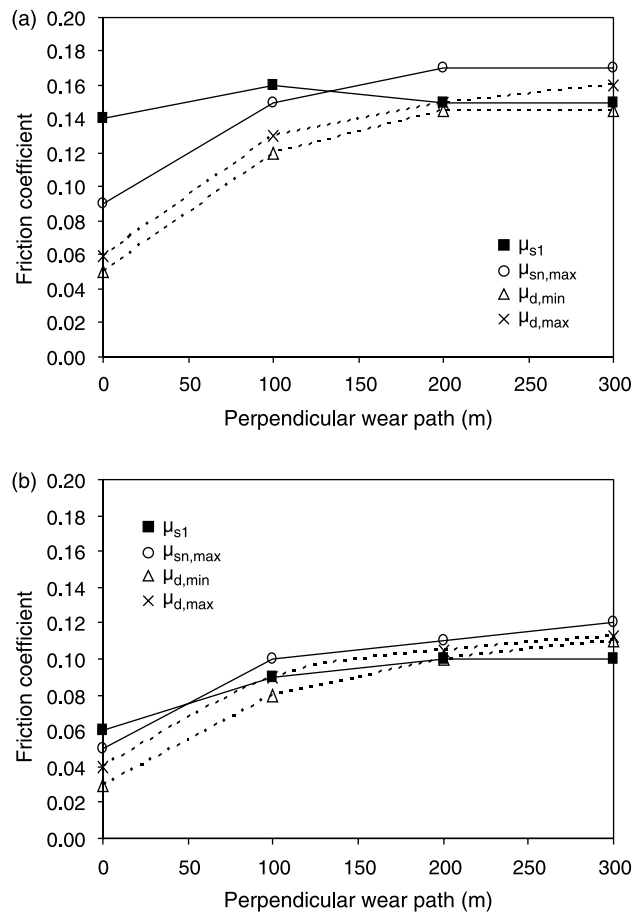


Fig. 12. Effect of perpendicular sliding motion under 75 MPa on large-scale friction of hybrid UHMWPE pads, (a) friction under 15 MPa, (b) friction under 30 MPa, ■ μ_{s1} , ○ $\mu_{sn,max}$, △ $\mu_{d,min}$, × $\mu_{d,max}$.

Table 9

Design values for friction coefficients of hybrid UHMWPE-pad/Zn-phosphate coating, applied to the high-loaded ball-joint

p (MPa)	Test results for maximum friction			Design values for friction		
	μ_{s1}	$\mu_{sn,max}$	$\mu_{d,max}$	$\mu_{G;d}$	$\mu_{L;s1;d}$	$\mu_{L;sn;d}$
15	0.21	0.17	0.16	0.22	0.26	0.21
150	0.03	0.03	0.02	0.03	0.04	0.04

distribution over the entire steel construction and sliding surfaces are considered:

- The global design criterion for friction does not assume that each of the pads is simultaneously subjected to maximum static friction, but roll and slip motion of the ball-joint causes 80% of the pads under dynamic sliding and 20% of the pads to break from the ball counterface and overcome static friction. The global design value of friction $\mu_{G;d}$ is estimated from Eq. (3):

$$\mu_{G;d} = \gamma_m(0.80\mu_{d,max} + 0.20\mu_{s1}) \quad (3)$$

- The local design coefficient of friction considers the maximum frictional force on one single hybrid UHMWPE-pad during the first sliding pass (Formula (4)) and subsequent sliding passes (Eq. (5)).

$$\mu_{L;s1;d} = \gamma_m\mu_{s1} \quad (4)$$

$$\mu_{L;sn;d} = \gamma_m\mu_{sn} \quad (5)$$

Coefficients of friction used for design of the ball-joint are evaluated in Table 9, revealing that global values are below the design limit of $\mu_{G;d} < 0.25$. Present solution thus fits the strength requirements implied by the steel structure. It was however shown in Fig. 6(a) that UHMWPE/Zn-coating contacts have a considerably long running-in phase and high initial static friction possibly occurs after wear and ageing of the coating (Fig. 12) during the first sliding step (floating). It was calculated that the contact stresses at a location on the back, front and bottom chairs during floating are however lower than the steady-state contact reported in Table 1: respectively, 7 MPa (back), 5 MPa (front) and 18 MPa (bottom). These imply lower stresses on the steel structures and allow for a higher local coefficient of friction (max. 0.50) on the bottom bearing without restrictions on strength.

The soft Zn-phosphate coating, initially developed for corrosion protection, provides extremely high wear resistance under high loads, reproduced on both tribotesters. From literature reviews [21], alternative ceramic or metallic coatings (stainless steels, TiN, Al,...) should yield application problems within a small working space ($\Delta R = 10$ mm) and the initial ball surface roughness $R_a = 3.2$ μm should be increased by blasting for proper adhesion. Present Zn-phosphate coating performs good adhesion under present roughness and 150 MPa contact pressure and it also provides lower friction under dry sliding compared to

steel, excluding the need and renewal of external lubrication. The surface undulations on the UHMWPE sliding pads are however maintained as a safety design factor for retaining eventual third bodies under failure. In case of coating wear, it has been observed that small cracks disappear under high-load sliding, possible due to local plastification under high flash temperatures. If wear however should occur, it has been verified that the bare steel counterfaces provide suitable running properties. Despite the climate conditioned environment, corrosion of the steel ball was previously observed on-the-field, leading to unacceptable corrosion particles in the sliding interface. Therefore the coating should be revised and periodically repaired, paying attention to the application method of the renewed coating, as illustrated in Table 4.

The UHMWPE sliding surface shows no wear after sliding against a Zn-coating, however deformations should be carefully analysed. Thickness reduction through combinations of wear and visco-elastic indentation should avoid contact between the steel bearing elements. After specification of the lip diameter, it flows regularly over the carbon ring leading to an increase in thickness at the borders after removal of the load. Sliding instabilities or coating removal during initial contacts in subsequent floating actions should be avoided by allowing free space (theoretical between 1 and 3.5 mm) between the front scale and sliding pads on the front chair or the back scale and sliding pads on the back chair, respectively. Therefore, both scales were in situ modified by a fillet on the running-in edges allowing for a progressive build-up of the contact pressures under sliding. This was simulated on a separate running-in test without damage observed on the UHMWPE pad nor on the Zn-coating. As shown in Table 5, the small tolerances between the hole and the pad diameter implies that the bottom diameter of the pad completely flows into the hole, additionally influencing its thickness and the difference in curvature radii between convex and concave bearing elements. In case of a positive or negative tolerance of the machined holes on the chair structures own to the fabrication process, the diameter of the UHMWPE pad should be modified within a narrow range. The rubber ring seems effective in retaining the pads within their holes, even under gravity when positioned on top of the chairs (simulation top specimen in tribotester Fig. 4(a)). The centered hole into the UHMWPE disc does not flow under shear and allows for removal of the polymer pads by air pressure in case of replacement. The relative position

between pad and counterface does not affect the wear resistance of the sliding pair.

5. Conclusions

A new design for the sliding surfaces in a ball-joint transmitting a total horizontal force of 350×10^6 N, has been achieved by incorporation of hybrid UHMWPE pads with a carbon fibre/epoxy reinforcing ring sliding against a Zn-phosphate coated counterface. It has been demonstrated by inter-laboratorial large-scale sliding tests, simulating the influences of creep and intermediate sliding paths, that the global design coefficient of friction (0.25) is not exceeded under dry sliding and the soft coating, initially applied for corrosion resistance, has extremely high wear resistance. However, direct contact between the carbon fibre/epoxy should be avoided by cold-flow of the polymer lip. Thermal analysis shows that the bulk temperature remains below the polymer softening point and local flash temperatures are below the melting point. However, the thermal stability of the coating is locally exceeded, possibly explaining a self-repairing action of slight cracks by plastification.

Acknowledgements

The authors express their gratitude to Solico B.V. and the Ministry of Transport, Public Works and Water Management (The Netherlands), allowing to present the test results and to be involved in the redesign of the Maeslant storm surge barrier.

References

- [1] Leendertz JS, Van Schepdael L, Van Paeppegem W, Samyn P, De Baets P, Degriek J. Modification of the ball bearing of the storm surge barrier near Rotterdam (NL). *Stahlbau* 2005 (submitted).
- [2] Franklin SE. Wear experiments with selected engineering polymers and polymer composites under dry reciprocating sliding conditions. *Wear* 2001;251:1591–8.
- [3] Collier JP, Mayor MB, McNamara JL. Analysis of the failure of 122 polyethylene inserts from uncemented tibial knee components. *Clin Orthop Rel Res* 1991;273:232–42.
- [4] Buechel FF, Pappas MJ, Makris G. Evaluation of contact stress in metal-backed patellar replacements. *Clin Orthop Rel Res* 1991;273:190–7.
- [5] Bartel DL, Bicknell VL, Wright TM. The effect of conformity, thickness and material stresses in UHMWPE components for total joint replacement. *J Bone Joint Surg* 1986;68A:1041–51.
- [6] Hayes WC, Lathi VK, Takeuchi TY. Patello-femoral contact pressures exceed the compressive yield strength of UHMWPE in total knee replacements. *Trans 39th ORS* 1993;421.
- [7] Ticona GmbH. Ultra high molecular weight polyethylene: product catalogue GUR 2002; p. 4–7.
- [8] Young SK, Lotito MA, Keller TS. Friction reduction in total joint arthroplasty. *Wear* 1998;222:29–37.
- [9] Nishimura I, Yuhta T, Ikubo K, Shimooka T, Murabayashi S, Mitamura Y. Modification of the frictional surfaces of artificial joints. *ASAIO J* 1993;762–6.
- [10] Benabdallah H. Friction and wear of blended polyoxymethylene sliding against coated steel plates. *Wear* 2000;254:1239–46.
- [11] Yamaguchi Y. *Tribology of plastic materials Tribology series 16*. Amsterdam: Elsevier; 1990.
- [12] Samyn P, De Baets P, Van Paeppegem W, Van Schepdael L, Suister E, Leendertz JS. Design of a Carbon/Epoxy reinforcing ring reducing creep of UHMWPE in high-loaded sliding contacts. Proceedings on 8th international conference on tribology, Veszprem (Hungary) 2004; p. 89–96.
- [13] Uetz H, Wiedemeyer J. *Tribologie der polymere (in German)-Tribology of polymers*, ISBN 3-446-14050-6, Carl Hanser Verlag, München/Wien, 1985.
- [14] Pascoe MW, Tabor D. The friction and deformation of polymers. *Proc Roy Soc London* 1955;A235:210–24.
- [15] Quintelier J, Samyn P, Ost W, De Baets P, De Baets T. The influence of scratched steel counterface on friction and wear lifetime of UHMWPE. Proceedings on 8th international conference on tribology, Veszprem (Hungary) 2004; p. 69–76.
- [16] Chang DCM, Goh JCH, Teoh SH, Bose K. Cold extrusion deformation of UHMWPE in total knee replacement prostheses. *Biomaterials* 1995;A6:219–23.
- [17] Dunaevsky VV, Booser ER, editors. *Tribology data handbook*. New York: CRC Press; 1997. p. 462.
- [18] Lee KY, Pienkowski D. Reduction in the initial wear of UHMWPE after compressive creep deformation. *Wear* 1997;203–204:375–9.
- [19] Turell M, Wang A, Bellare A. Quantification of the effect of cross-path motion on the wear rate of UHMWPE. *Wear* 2003;255:1034–9.
- [20] Wang A. A unified theory of wear for UHMWPE in multidirectional sliding. *Wear* 2001;248:38–47.
- [21] Holmberg K, Matthews A, Ronkainen H. Coatings tribology-contact mechanisms and surface design. *Tribol Int* 1998;31(1–3):107–20.